The Mechanistic Process Analysis and Temperature Effect in a Low Pressure Square Type Atomic Layer Deposition Reactor

Rigardt Alfred Maarten Coetzee, Tien-Chien Jen, and Muaaz Bhamjee
Department of Mechanical Engineering Science, University of Johannesburg, Johannesburg, Auckland Park 2006, South Africa
Email: tjen@uj.ac.za

Junling Lu
Department of Chemical Physics, University of Science and Technology of China, Baohe District, Hefei 230026, China

Abstract—**This work studies the fundamental operation behaviour of the nano thin film manufacturing process called atomic layer deposition. This attractive key-enabling nanotechnology is well known to deposit ultrathin, uniform, conformal and pinhole-free nano-films on complex topography. It is used in microelectronics, solar cells, food packaging, fuel cells, and water purification systems, among other applications. However, the technology is facing an impasse in providing detailed information on the understanding of the ALD process. With numerical simulations, this study investigates the internal mechanical behaviour and the growth rates in the Al2O3 thin film ALD process influenced at temperatures of 200 ℃ and 250 ℃. TMA and O3 precursors with argon gas as the purge substance are used to examine an arbitrary Gemstar 6 ALD reactor. The governing laws of the conservation of mass, momentum, energy, species, and kinetic chemical reactions are analysed in a continuum domain, by using the software ANSYS Fluent and ChemkinPro. The results were validated by available literature and good agreement was achieved.**

Index Terms—**advance manufacturing, nanotechnology, atomic layer deposition, ultra-thin film**

I. INTRODUCTION

Atomic layer deposition (ALD), has received wide recognition as an attractive key-enabling nanotechnology for depositing ultrathin, uniform, conformal and pinhole-free nano-films on complex topography [1, 2]. In the past few decades, ALD had been implemented extensively in both silicon microelectronics and thin film device industries, and is rapidly expanding to more industrial applications [3, 4]. This technology serves a greater potential in future manufacturing and research applications showing extensive development in the manufacturing of nanoscale devices [5, 6]. This deposition process consists of being a binary reaction that is divided into self-limiting surface reactions between the gaseous precursors, and the absorbed species on a substrate [7-10]. Basically, the ALD procedure involves firstly, exposing the surface of the substrate to the first precursor, which saturates the surface. Thereupon, the excess precursor and volatile by-products are purged from the reactor. The adsorbed layer is then introduced to react with the second precursor, and the volatile by-products and excess of the second precursor are purged from the reactor again [11]. These steps are illustrated in the schematic in Fig. 1 (a). By repetition of these saturate steps, the thin film can be grown layer-by-layer [9]. Due to the film growth being self-limiting, the film thickness can be precisely controlled to produce uniform and conformal thin films [11].

The ALD method has facilitated a process in which highly reactive species and low process temperature can be utilized to fabricate metal oxide films. Before ALD, these films were extremely difficult to deposit [11]. For this reason it has become of great interest in new industrial applications, such as diffusion barriers, superconductor layers in quantum qubits, and fuel cell technology. But the fabrication of films for these industrial products demands efficient low temperature, and defect-free ALD processes. Aluminium oxide (Al_2O_3) film is of interest in this work due to the fact that many current industrial applications, future potential applications, as well as early applications are based on Al_2O_3 thin films. The use of trimethylaluminium (TMA) and ozone (O_3) as precursors with argon gas to purge substance is selected for this study. Ozone as precursors exhibits in many instances similar attributes to oxygen plasma, as it produces a copious supply of highly reactive oxygen atoms. When ozone decomposes it produces stable oxygen molecules, as well as oxygen atoms. In either case, the oxygen atoms are highly reactive, and readily decompose the TMA.
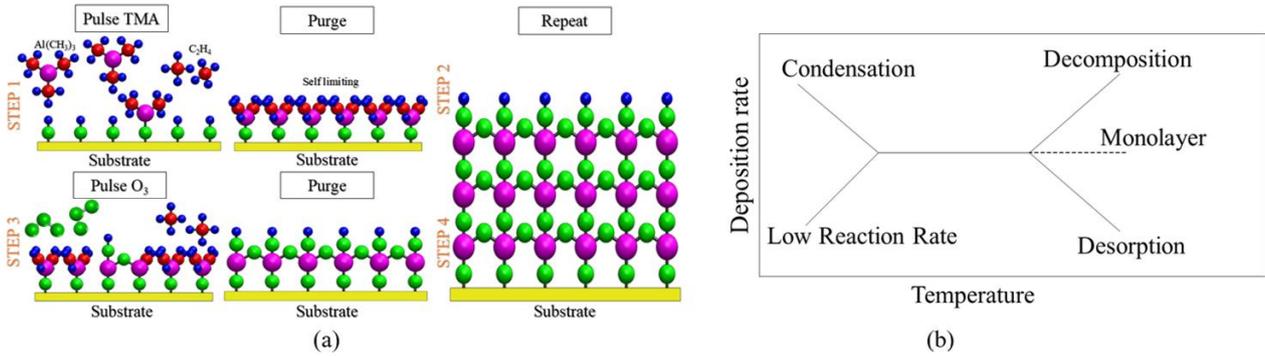
Figure 1. (a) Atomic layer deposition procedure schematic (author's own illustration), (b) the typical deposition rate vs temperature window.

Thermal ALD processes are thermally constrained on the feasibility of successfully depositing particular films. In an instance of low temperature, the deposition rate might show higher than expected values due to physical condensation occurring. The temperature can be too low and not energize enough reaction to occur on the substrate. At high temperature instances the film may desorb before the introduction of the next reactant precursor. Similarly, high temperature can also decompose the film entirely [11]. This can be seen in the temperature window schematic in Fig. 1 (b). Al_2O_3 film can be deposited across a relatively wide temperature window. Although this is said, the process characteristic within ALD reactors to predict these influences is not yet well understood. As such, this study numerically investigates the temperature effects of 200 °C and 250 °C, on the mass fractions, deposition rate, and surface mechanistic behaviour of a single cycle. This is accomplished by simulating an arbitrary Gemstar 6 square type ALD reactor via computational fluid dynamics with the software ANSYS Fluent 18.2 and ChemkinPro 18.2.

II. MATHEMATICAL MODEL

The ALD process mathematical model consists of coupling and decoupling steps. First, the physical and chemical processes are decoupled. The physical processes consisting of the governing equations of conservation of mass, momentum, energy, and species transport is decoupled from the chemical reactions. These processes are presented by corresponding partial differential equations (PDEs) that are solved numerically on defined nodes in the mesh domain. Second, the PDE processes are coupled to obtain the entirety of the ALD numerical solution by taking into account the interactions between each physical and chemical process. These modelling steps governing equations are expressed as:

$$\frac{\partial \rho}{\partial t} + \nabla \cdot (\rho \vec{v}) = S_m \tag{1}$$

$$\frac{\partial \rho \vec{v}}{\partial t} + \nabla \cdot (\rho \vec{v} \vec{v}) = -\nabla P + \nabla \cdot \tau + \rho \vec{g} + \vec{F} \tag{2}$$

$$\frac{\partial \rho E}{\partial t} + \nabla \cdot (\vec{v}(\rho E + \rho)) = \nabla \cdot (k_{eff} \nabla T - \sum h_i J_i) + R_r \tag{3}$$

$$\frac{\partial (\rho Y_i)}{\partial t} + \nabla \cdot \rho \vec{v} Y_i = -\nabla \cdot \vec{J_i} + R_i \tag{4}$$

where J, $keff$ and R resembles the diffusion term, effective conductivity, and reaction source term, respectively.

The rth irreversible surface reaction can be shown as the following general form:

$$\sum_{i=1}^{N_g} g'_{i,r} G_i + \sum_{i=1}^{N_b} b'_{i,r} B_i + \sum_{i=1}^{N_s} s'_{i,r} S_i = \sum_{i=1}^{N_g} g''_{i,r} G_i + \sum_{i=1}^{N_b} b''_{i,r} B_i + \sum_{i=1}^{N_s} s''_{i,r} S_i \tag{5}$$

Where G, B and S corresponds to the gaseous species, the bulk species, and the site species, respectively. The molar reaction rate for the irreversible surface reaction can be calculated as follows:

$$R_r = k_{f,r} (\prod_{i=1}^{N_g} [C_i]_{wall}^{\eta'_{i,gr}})(\prod_{i=1}^{N_s} [S_j]_{wall}^{\eta'_{i,sr}}) - k_{b,r} (\prod_{i=1}^{N_g} [C_i]_{wall}^{\eta''_{i,gr}})(\prod_{i=1}^{N_s} [S_j]_{wall}^{\eta''_{i,sr}}) \tag{6}$$

This follows that the mass deposition rate $(\dot{m}_{dep})$ can be obtained at the substrate surface as:

$$\dot{m}_{dep} = \sum_{i=1}^{N_b} M_{w,i} \hat{R}_{i,bulk} \tag{7}$$

III. SIMULATION ENVIRONMENT

An arbitrary Gemstar 6 reactor is designed to duplicate and represent similar working principals. The simulation domain is meshed into a grid of 28 966 nodes and 69 743 cells. The reactor is designed to illustrate the top half of the actual reactor having a volume to surface area ratio off 883.18 cm^3/1585.54 cm^2. The design and mesh grid is illustrated in Fig 2.
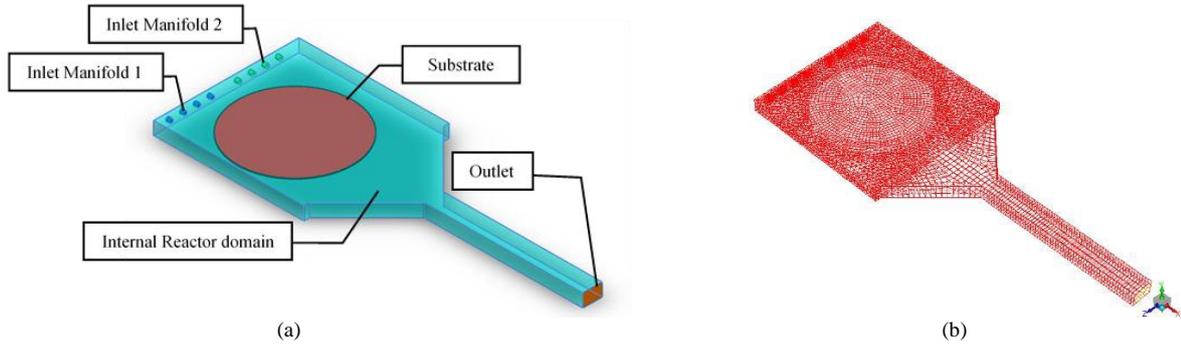
Figure 2. Arbitrary Gemstar 6 reactor: (a) reactor with substrate, inlet manifold 1 & 2, internal reactor domain and the outlet condition 1, and (b) the meshed reactor domain.

The precursors are injected sequentially into the reactor with an operating pressure of 1 torr to flow and react over the 150 mm substrate. The substrate and reactor walls are heated to 200 ℃ or 250 ℃, respectively, while the inlets are kept at 150 ℃. The manifold activation sequence, injection time and inlet velocity are shown in Table I.

TABLE I. INPUT PARAMETERS AND OPERATION SEQUENCE

Gases	Manifold sequence	Injection time (seconds)	Velocity (m/s)
Argon (pre-purge)	1&2	5	0.02
TMA	1	0.2	0.02
Argon	1&2	5	0.02
Ozone	2	0.2	0.02
Argon	1&2	5	0.02

The finite volume approach is discretized spatially and temporally using second order upwind and first order implicit methods, respectively. The transport equations source terms are linearized and the pressure- velocity components are solved by the robust PISO algorithm solver for the transient case. Solution residuals are monitored and considered converged when the continuity, velocity and temperature components are less than 1×10^{-5}, and less than 1×10^{-4} for the species. A User Define Function (UDF) is created to simulate the sequential process at a time step of 5×10^{-5} seconds.

IV. RESULTS

At the moment TMA is introduced in the 5 seconds pre-purged argon gas reactor domain; the flow protrudes over the substrate area at an offset angle as the mass fraction is growing through the pulse time from the manifold 1 location. After the pulse sequence of TMA, both manifolds introduce argon purge time in which the angled flow is slowly rectified to a more vertical sweep. At about 8.4 seconds, the argon gas wall reaches the substrate and starts to reveal the buffer layer of TMA still passing over the substrate. However, the purging time is not long enough to purge the entire quantity of TMA out of the reactor. When the O_3 is pulsed into the domain of manifold 2, a carrier argon buffer layer is formed.
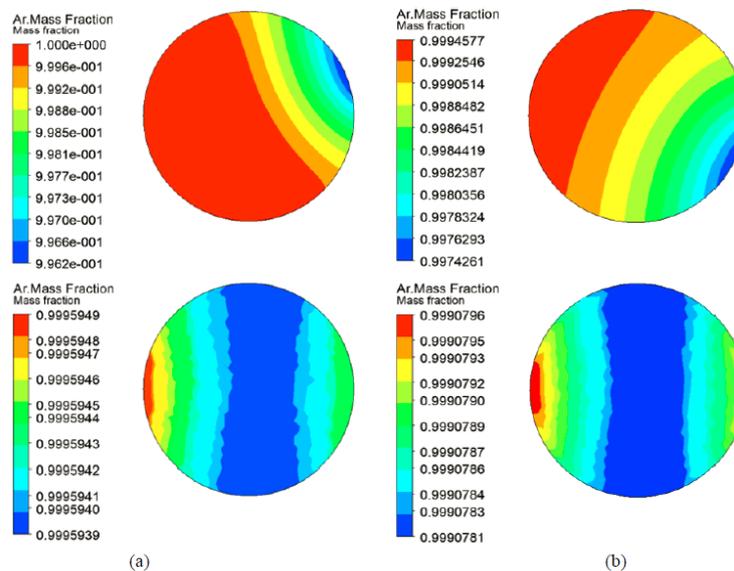

Figure. Argon mass fraction illustrating substrate coverage: (a) TMA coverage over the substrate of 5.2 seconds (top), and 9 seconds (bottom) and (b) O3 coverage over the substrate of 10.4 seconds (top), and 12.5 seconds bottom).

Similarly to the TMA half-cycle sequence, O_3 forms an offset flow over the substrate, but at the mirrored position to that of TMA. This is again rectified at a much faster pace than TMA when argon is introduced out of both manifolds at the next purging sequence. At about 12.1 seconds the O_3 buffer layer is revealed. Sequences to illustrate these mechanistic behaviours are illustrated in Fig. 3.

Due to the purging times not being sufficient to purge the gas out of the domain, the domain consists entirely of all three gas sources (TMA, argon, and O_3) along with the reaction gasses and emissions still within the reactor. These situations are adverse for ALD processes, as this may lead to gaseous homogenous reactions among the precursors when the argon buffer layer thickness is not

sufficient to divide the reactive precursors. This can result in significant defects within the fabricated thin film. Furthermore, along the TMA and O3 buffer layers, intensive flow distortions are observed through time. These distortions are believed to be caused by the surface reactions producing emissions and the reaction gases.

The mass fraction cycle trend of the pulsed TMA and O_3 precursors along with the Al_2O_3 deposition rates at 200 ℃ and 250 ℃ along the substrate is illustrated in Fig. 4. The pulsed and purge sequences are divided by vertical dash-dot lines and consequently, the behaviour of these parameters can be visualized along the pulse-purge-pulse-purge cycle.
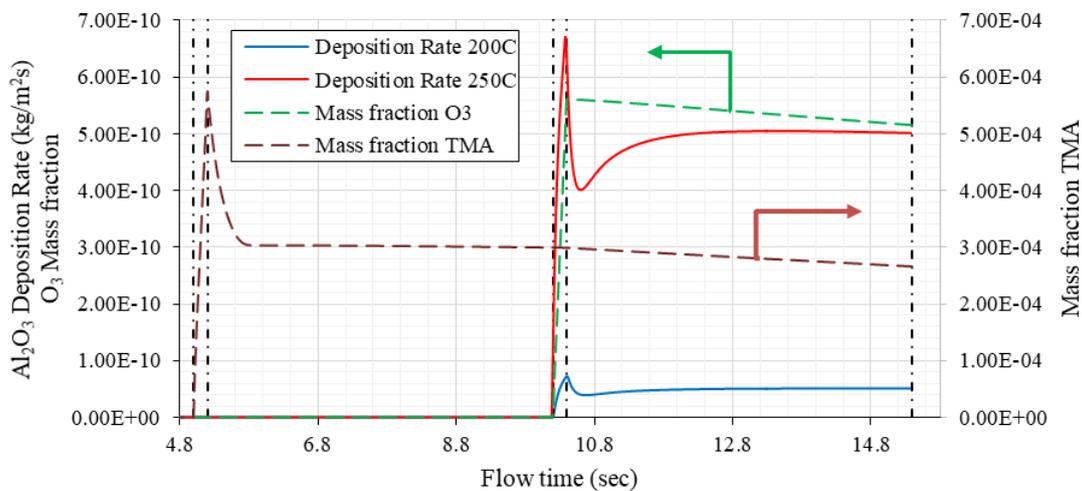

Figure 4. Al2O3 deposition rate at 250 ℃ and 200 ℃ along with the O3 and TMA mass fraction at 250 ℃ for one ALD cycle.

At the first TMA pulse (between 5-5.2 second) it is seen that TMA drastically increases, are satisfied and decreased along the argon purging sequence. At some stage the TMA mass fraction equalizes as at this point, due to the TMA not being able to be purged out completely, the domain contains the full amount of TMA in ratio with the old and new purge argon buffer layers. The TMA mass fraction is again influenced and results in another decrease as O_3 is pulsed and accompanied by another purge.

In the O_3 pulse (between 10.2-10.4 second) the mass fraction of this precursor significantly increases, but does not satisfy as the TMA does, revealing that more time should have been given to this oxidizer. Intrinsically, at this moment this precursor is linked to the surface reaction on the substrate, and an Al_2O_3 thin film is deposited. Along with the gaseous reaction, surface reaction and emissions the O_3 mass fraction decreases at a steady gradient along the purging sequence.

Contained by Fig. 4 the deposition rate reveals a steep increase within the O_3 pulse, peaking at a growth rate of 0.915 Å/cycle at 250 ℃. These growth rates are comparable to those found in the literature [1, 2, 9, 10], as well as what is typically expected for this ALD thin

film recipe. Intrinsically, steeper slopes of the deposition curves for the hotter substrate indicate earlier film depositions and result in a larger surface reaction rate constant along with a faster substrate oxidation. However, this also leads to higher amounts of emissions generated.

V. CONCLUSION

The mechanistic process and temperature effect in a low pressure square type ALD reactor are analysed for an arbitrary Gemstar 6 ALD reactor fabricating Al_2O_3 thin film at 200 ℃ and 250 ℃. The thin film is deposited unto a substrate in sequence by pulsing and purging TMA, ozone and argon, respectively, through 8 inlet, spliced manifold. A single cycle mechanistic flow reveals buffer layers of the precursor and purge substances simultaneously within the reactor. These instances can lead to adverse results for ALD processes, such as gaseous homogenous reactions among the precursors when the argon buffer layer thickness is not sufficient to divide the reactive precursors, and ultimately create defects within the fabricated thin film. Intrinsically intensive flow distortions were observed, believed to be caused by the surface reactions produced

by the emissions and reaction gases. Thereupon, the mass fraction along the entire cycle was observed along with the deposition rate that revealed steeper slopes for the hottest reaction process. A growth rate of 0.915 Å/cycle @ 250 ℃ is recorded that benchmarked previous results. Hence, this paper serves as a means to guide future research efforts in the field of ALD process investigation.

REFERENCES

[1] D. Pan, "Numerical and experimental studies of atomic layer deposition for sustainability improvement," *Doctor of Philosophy in Engineering. Department of Engineering*, University of Wisconsin. Milwaukee, USA; 2016.

[2] D. Pan, L. Ma, Y. Xie, T. C. Jen, C. Yuan, "On the physical and chemical details of alumina atomic layer deposition: A combined experimental and numerical approach," *Journal of Vacuum Science & Technology A*, 2015, vol. 33, no. 2, pp. 021511.

[3] S. M. George, "Atomic layer deposition: An overview," *Chemical Reviews*, vol. 110, no. 1, pp. 111-131, 2010.

[4] R. A. M. Coetzee, W. S. Ebhota, T. C. Jen, "Numerical modelling in the atomic layer deposition process: A short review," *Submitted to Molecular Simulation*, 2017.

[5] Bohr MT SM, R. S. Chau, T. Ghani, K. Mistry, "The high-k solution," *IEEE Spectrum*, vol. 44, no. 1, pp. 29-35, 2007.

[6] V. Dwivedi, R. A. Adomaitis, "Multiscale modeling of atomic layer deposition processes," In: *American Control Conference*: 2009, pp. 2495–2500.

[7] C. R. Kin, J. Y. Lee, J. H. Heo, C. M. Shin, T. M. Lee, J. H. Park et al. "Effects of annealing temperature and Al$_2$O$_3$ buffer layer on ZnO thin films grown by atomic layer deposition," *Current Applied Physics*, vol. 10, no. 1, pp. 298-301, 2010.

[8] J. Y. Kim, J. H. Ahn, S. W. Kang, J. H. Kim, "Step coverage modeling of thin films in atomic layer deposition," *Journal of Applied Physics*, vol. 101, no. 1, pp. 073502, 2007.

[9] M. R. Shaeri, T. C. Jen, C. Y. Yuan, "Reactor scale simulation of an atomic layer deposition process," *Chemical Engineering Research and Design*, vol. 94, no. 1, pp. 584-593, 2015.

[10] M. R. Shaeri, T. C. Jen, C. Y. Yuan, "Improving atomic layer deposition process through reactor scale simulation," *International Journal of Heat and Mass Transfer*, vol. 78, no. 1, pp. 1243-1253, 2014.

[11] J. Hämäläinen, M. Ritala, M. Leskelä, "Atomic layer deposition of noble metals and their oxide," *Chemistry of Materials*, 2014, vol. 26, no. 1, pp.786-801

Prof. Tien-Chien Jen is a professor in the Department of Mechanical Engineering Science in the School of Mechanical and Industrial Engineering at the University of Johannesburg in South Africa. His current interest centers on cutting-edge hydrogen energy generation and storage. Topics range from constructing a hydrogen-powered ATV to finding novel materials and techniques to coat fuel cells to increase electron conversion efficiency. Dr. Jen has also acquired extensive administrative experience, as the Interim Dean of the College of Engineering and Applied Science at the University of Wisconsin – Milwaukee and as Dean of the College of Engineering at the University of Alaska Anchorage. His varied and numerous accomplishments include establishing the new Engineering and Industrial building, establishing and strengthening industrial partnerships with local companies, such as ConocoPhillips and BP, and obtaining multimillion-dollar commitments for scholarships and equipment requisitions. He has also championed diversity and has actively encouraged traditionally underrepresented minorities to major in Engineering. Dr. Jen's home page: http://www.tienchienjen.com/.

Mr. Rigardt A.M. Coetzee is currently a PhD candidate under the supervision of Prof Tien-Chien Jen. He was awarded meritorious student of 2014 in the field of Mechanical Engineering from SAIMeCHE. His research is based on the understanding of the ALD process, reactor design and thin film simulation methods. Furthermore, his research expertise also extends to renewable energy systems. He has published peer-reviewed journals concerning solar thermal systems and multi-purpose solar thermal systems in accredited journals. Mr. Coetzee also contributes to the renewable energy projects and advance manufacturing processes such as the solar car challenge, cold gas dynamic spray, dry drilling, among others at the University of Johannesburg. Mr. Coetzee's Email: rcoetzee@uj.ac.za

Dr. Muaaz Bhamjee is presently a Senior Lecturer and in the Department of Mechanical Engineering Science at the University of Johannesburg. His research interests are in investigating various CFD modelling techniques, namely Navier-Stokes and Lattice Boltzmann based methods, for hydrocyclones and other multiphase flow equipment. The ultimate aim of this research is to improve the understanding of the physics of such flows and to provide accurate and computationally efficient models to be used in design optimization of mineral processing processes and equipment. Dr. Bhamjee's Email: muaazb@uj.ac.za

Prof. Junling Lu obtained his B.S. degree in Henan University in 2002 and his Ph. D in condensed mater of physics under the supervision of Prof. Hongjun Gao in Institute of Physics, CAS in 2007. In 2012, he received the award of the One Thousand Young Talents Program under the Recruitment Program of Global Experts. In March 2013, He became a professor in University of Science and Technology of China. His main research interest is in atomically-precise design of new catalytic materials using a combined wet-chemistry and atomic layer deposition (ALD) method. Dr. Lu's Email: junling@ustc.edu.cn